A Density Functional Study of the Chemical Differences between Type I and Type II MoS_2-Based Structures in Hydrotreating Catalysts†

Berit Hinnemann*,‡ Jens K. Nørskov,‡ and Henrik Topsøe*,§

Center for Atomic-scale Materials Physics, Department of Physics, Building 307, Technical University of Denmark, DK-2800 Lyngby, Denmark and Haldor Topsøe A/S, Nymøllevej 55, DK-2800 Lyngby, Denmark

Received: March 15, 2004; In Final Form: June 7, 2004

Density functional theory is used to investigate the origin of the activity differences between Type I and Type II MoS_2-based structures in hydrotreating catalysts. It is well known that the Type II structures, where only weak interactions with the support exist, have a higher catalytic activity than Type I structures, where Mo−O linkages to the alumina are present. The present results show that the differences in activities for MoS_2 and Co−Mo−S structures can be attributed to the electronic and bonding differences introduced by the bridging O bonds. We find that the Mo−O linkages are most probably located on the $(\bar{1}010)$ S edge. The presence of oxygen linkages increases the energy required to form sulfur vacancies significantly so that almost no vacancies can be formed at these and neighboring sites. In this way, the reactivity of the S edge is reduced. In addition, the studies also show that the linkages introduce changes in the one-dimensional metallic-like brim states. Furthermore, the presence of oxygen linkages also changes the energetics of hydrogen adsorption, which becomes less exothermic on sulfur sites directly above linkages and more exothermic on sulfur sites adjacent to linkages. The present results explain previously observed differences in Type I−Type II transition temperatures for Co−Mo−S structures with different Co contents.

1. Introduction

The role of support interactions has for many years been a central topic in catalysis research. Most of the early work has dealt with supported metal catalysts (see, e.g., ref 1), but more recently these investigations have also been extended to the study of supported sulfides (see, e.g., refs 2 and 3). Such catalysts have for many years been used as hydrodesulfurization (HDS) catalysts, but with the recent emphasis on the production of ultralow sulfur diesel (ULSD), and other clean transport fuels,[4−7] special focus has been devoted to the development of improved catalysts and to the understanding of how one can use support interactions to produce catalysts with desired catalytic properties.

Most of the studies of HDS catalysts have dealt with alumina-supported Co−Mo or Ni−Mo catalysts that are most widely used in industry. Several parameters influence the activity of $Co-Mo/Al_2O_3$-type catalysts. One is the MoS_2 edge dispersion since this determines the potential capacity to accommodate the promoter atoms at the edges of MoS_2 in the form of the active Co−Mo−S structures.[2] The use of alumina as a support is advantageous in this regard since it allows the production of small stable nanoclusters of MoS_2.[8] The intrinsic catalytic properties of the MoS_2 and Co−Mo−S structures may also be influenced by the support. For example, Candia et al.[9] observed that increasing the sulfiding temperature from 673 to 873 K resulted in the formation of modified Co−Mo−S structures (termed Type II Co−Mo−S) which had a substantially higher intrinsic activity than those formed at the lower temperatures (termed Type I Co−Mo−S). It was suggested[9] that the low activity of Type I Co−Mo−S is caused by the presence of some Mo−O−Al linkages between the MoS_2 and the alumina support. The presence of such species in sulfided catalysts may be related to the strong tendency for Mo to interact with surface alumina OH groups during catalyst preparation and form highly dispersed monolayer type structures,[10−13] where Mo is most difficult to sulfide and reduce. The interactions are strongest for low Mo surface coverages.[14,15] In this concentration region, Mo interacts preferentially with basic OH groups.[10−13] FTIR studies of the same catalysts before and after sulfiding showed that the Mo−O−Al linkages, which remain intact after sulfiding, originate from the interaction with the basic OH groups.[13] ESR[16] and XPS[17] results have revealed the presence of oxo-Mo^{5+} species which were attributed to the linkages with the alumina support. Evidence for such linkages in Type I structures has also been obtained from EXAFS[18] and inelastic tunneling spectroscopy studies.[19] Mössbauer emission spectroscopy studies showed no observable differences in the nature of the Co atoms in Type I and II Co−Mo−S structures.[20,21] Thus, these results also show that the support interactions involve the Mo atoms and not the promoter atoms. This is supported by the observation that supported nonpromoted MoS_2 catalysts may also be present in the Type I and Type II forms.[22]

The more active Type II species can, as already mentioned, be generated by breaking the Mo−O−Al linkages by sulfiding at high temperatures. This has the disadvantage that the overall MoS_2 edge dispersion will decrease[9] and alternate procedures are therefore desirable. It has been shown that by the introduction of additives or chelating ligands one may circumvent the formation of the less active Type I structures and generate directly Type II Co−Mo−S.[21,23−25] Another procedure is to use supports which only weakly interact with the Mo species. It has, for example, been shown that the Co−Mo−S structures

† Part of the special issue "Michel Boudart Festschrift".

* Corresponding authors. Henrik Topsøe e-mail: het@topsoe.dk; Berit Hinnemann e-mail: Berit.Hinnemann@fysik.dtu.dk.

‡ Center for Atomic-scale Materials Physics.

§ Haldor Topsøe A/S.

10.1021/jp048842y CCC: $30.25
Published on Web 08/04/2004

formed in carbon-supported catalysts[26,27] exhibit Type II-like activity behavior.[20] Also, high activity unpromoted Type II MoS_2 structures are readily formed on carbon supports.[28] Silica is another support that may yield Type II structures.[29]

Several microscopy studies[2,30−34] have focused on obtaining insight into how the MoS_2 structures are bonded to the alumina support. Using single-crystal alumina surfaces, Sakashita et al.[32] showed that the perpendicular (or near perpendicular) edge bonding of MoS_2 sheets dominate on the (100) γ-Al_2O_3 surface, whereas the basal plane bonded morphology dominates on (111) surfaces. For typical catalysts prepared using high surface area amorphous alumina supports, the flat bonding via the MoS_2 basal planes appears to dominate.[2] Many studies have shown that catalysts containing Type II Co−Mo−S contain multistack MoS_2 structures. This does, however, not appear to be an essential prerequisite for the formation of Type II structures and single-slab Type II Co−Mo−S samples may be produced.[2,17]

The origin of the low activity of Type I structures is not well understood and several factors may play a role. It has been suggested[28] that the interaction with the support via oxygen bridges for the Type I structures leads to a polarization of the Mo−S bonds, a decrease in their covalent character, and thus an increase in the Mo−S bond strength. According to the bond energy model, this is not desirable for the activity.[35] It is also expected that the degree of stacking of MoS_2 layers may influence the catalytic properties. This may be related to steric constraints and different accessibility of reactants to edge sites in different layers of the stack.[36] For example, the bottom layer of a stack may be less active because of steric hindrance,[5] as also observed in other systems.[37] Furthermore, it is only the top MoS_2 layer that will expose the special brim sites observed in recent STM studies.[38] Such sites exhibit metallic character and were observed to be involved in hydrogenation reactions.[39] These reactions are of particular interest since deep HDS typically requires prehydrogenation of the aromatic rings in the very unreactive sulfur containing molecules.[5,40]

Recently, many theoretical studies using in particular DFT methods have contributed to the understanding of the intrinsic structure of MoS_2 and Co−Mo−S and how the important edge structures depend on the working conditions and on the adsorption of hydrogen and thiophene.[41−60] Generally, in these studies the MoS_2 is modeled either as a periodic structure in a unit cell or as a cluster. While periodic calculations are often very efficient, cluster calculations have the advantage that they can consider the effect of particle size and corners. The interaction between MoS_2 and alumina surfaces has also been addressed by molecular dynamics[19,61,62] and DFT methods.[63−65] The latter studies have favored a perpendicular (edge-bonded) orientation.

In the present paper, we present DFT studies aimed at understanding the origin of the intrinsic catalytic differences between Type I and Type II structures. As a starting point, we therefore neglect the effects of the morphological relationship between the sulfide structure and the support and instead concentrate on investigating to what extent the presence of Mo−O bonds in the sulfide structure may change the electronic and bonding properties of the sulfide. Oxygen linkages are introduced in different places of the structure. These results provide insight into the most likely location of the linkages to the support. The presence of linkages in the MoS_2 structure is observed to reduce the tendency to form vacancies at neighboring sites. In addition, the studies also show that the linkages introduce changes in the one-dimensional metallic-like brim states and their ability to interact with molecules of relevance for HDS. In this way, the studies provide insight into the origin of support-induced activity changes of MoS_2 and Co−Mo−S structures.

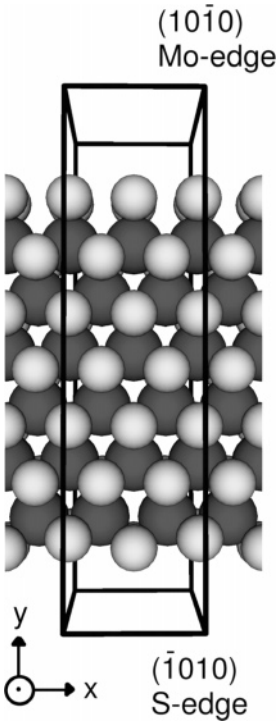

Figure 1. The employed model for MoS_2 in the density functional calculations. One unit cell is two units of MoS_2 wide and six rows of MoS_2 deep. Thus, both the Mo edge and the S edge are exposed.

2. Calculational Details

We perform density functional theory calculations with the program dacapo,[66] which uses a plane-wave expansion of the Kohn−Sham wave functions[67,68] and ultrasoft pseudopotentials.[69] We use a plane wave cutoff of 30Ry for all calculations. Furthermore, we use the double-grid technique,[70] where we set the electron density cutoff to 60Ry. This results into a high accuracy of the forces. The Kohn−Sham orbitals are populated according to the Fermi distribution with an electronic temperature of $k_BT = 0.1$ eV.[68] All energies have been extrapolated to zero electronic temperature. We sample the Brillouin zone by six *k*-points in the *x*-direction and by one *k*-point in the *y*- and *z*-directions.[71] For calculation of band structures and wave functions, we use 48 *k*-points in the *x*-direction to ensure a proper resolution. All calculations are performed with the Perdew-Wang 91 (PW91) exchange-correlation functional.[72]

The employed periodic model is shown in Figure 1. We use a unit cell, which is two units of MoS_2 wide and six rows of MoS_2 long. The equilibrium lattice constant for MoS_2 has been determined to be 3.215 Å. The unit cell comprises two Mo atoms in the *x*-direction. The length of the unit cell is 6.43 Å in the *x*-direction, 25 Å in the *y*-direction, and 12 Å in the *z*-direction. Thus, in the *y*-direction, the atoms of different images are at least 7.4 Å apart and in the *z*-direction at least 8.8 Å. Together with the employed dipole correction, these image separations have been tested to be sufficient for the interactions between the images to be negligible.

For a full model of the system, one would have to model the MoS_2 slab on an Al_2O_3 system. Modeling MoS_2 on the alumina support has been attempted,[19,61−65] but this is very complex and not at all straightforward. To make the system more tractable, we model the Mo−O−Al linkages as Mo−O−H groups. From

a chemical point of view, this is reasonable, as the oxygen is located in similar electron-donating surroundings. In the actual alumina support system, Al−O−Mo linkages can be formed from OH groups present on the alumina. In our model, we assume that the OH groups come from water instead (see also section 3.2). Our approximation depends on whether the OH groups are located in similar chemical surroundings and whether the bond strength of the OH group to alumina and to hydrogen is comparable. One measure for the bond strength and the chemical environment is the OH stretching frequency. On alumina support, the OH stretching frequency of the most basic OH groups, which preferentially interact with Mo, has been measured to be 3771 cm^{-1}.[12,13] Also, the other OH groups present on the alumina, which are less basic, interact with the Mo, and their frequencies have been measured to be 3730 cm^{-1} and 3684 cm^{-1}.[12,13] This value should be compared to the two stretching frequencies of the water molecule, which are 3657 cm^{-1} and 3756 cm^{-1}.[73] The OH stretching frequencies differ only slightly, which means that the bond strength within the OH group is approximately equal. Another OH stretch frequency available for comparison has been measured for hydroxyl groups on thin alumina films to be 3711 cm^{-1}.[74] Also, this frequency is close to the stretch frequencies of the water molecule. This shows that both for the Al−OH groups and for the Al−O−Mo linkages, the oxygen in our model is located in an environment, which is similar to the situation on the alumina support.

There are, of course, aspects of the alumina support, for example, lattice mismatch or rigidity, which we cannot include in our present model. Nonetheless, we can illustrate the chemical changes introduced by the alumina support and their consequences on structure and reactivity. Lattice mismatch might cause a deviation from the flat layer structures.[17,33] Investigating lattice mismatch effects requires a much more sophisticated model and remains a task for the future.

Also, we would like to stress that the main purpose is to obtain information on the electronic and chemical changes in the MoS_2 structures caused by the oxygen linkages. Our conclusions are based on energy differences of ∼50 kJ/mol and higher so that it is unlikely that small energy shifts due to the alumina would change them.

This model might also apply to other types of support. The key requirement is that the OH groups are located in similar chemical environments. Furthermore, our study provides information on water adsorption on MoS_2 surfaces.

3. Results and Discussion

3.1 Stability of OH Terminations. It is known from previous DFT calculations that under sulfiding conditions both the Mo edge and the S edge are most stable, when terminated with sulfur dimers (the exact stability depends on the ratio of the partial pressures of H_2 and H_2S, as discussed in refs 48, 51, 54, and 59). We use this for building our model, as shown in Figure 1. When we substitute some S atoms with OH groups in the following calculations, we always keep the edge which is not involved in the substitution at the energetically most stable dimer termination. We choose the dimer termininations as reference although under hydrodesulfurization conditions, the monomer configurations are expected to be present.[48,51,54,59] The reason for this is that, as we show later, the vacancy formation energy in the presence of the oxygen linkages is very high so that the structure with oxygen linkages and sulfur present is the most likely one, and this can only be compared to a dimer reference.

It was observed that vacancy formation on the Mo edge is energetically more expensive than vacancy formation on the S edge.[54] When the Mo edge is terminated with sulfur monomers, all sulfur atoms on this edge undergo a concerted reconstruction. Therefore, for extended Mo edges it is difficult to create single vacancies, as this stabilizing reconstruction is only possible when all atoms of the edge participate. On the sulfur edge, no such global reconstruction takes place, when creating a vacancy, and therefore this requires less energy than on the Mo edge.[54]

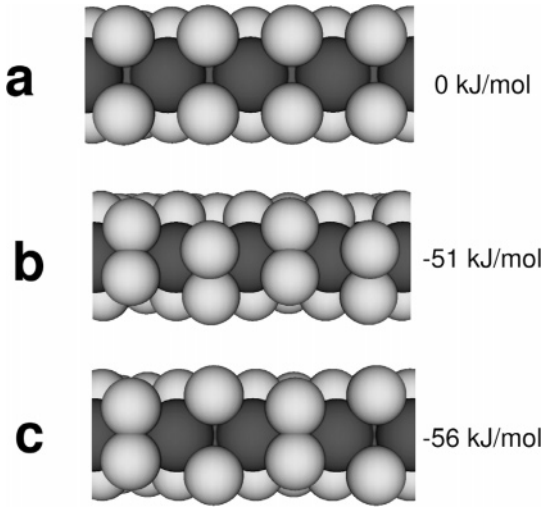

Figure 2. Three different edge terminations for the S edge. The energies are given in kJ/mol and per unit cell, i.e., per two units of MoS_2 (see Figure 1). The symmetric termination a is less stable than both reconstructed terminations b and c. The dimers in structure b are tilted in and out of the paper plane. The atoms are depicted as molybdenum (large, dark gray), sulfur (large, light gray), oxygen (small, gray) and hydrogen (small, white). This scheme is also used for Figures 3, 4, 5, and 7.

While it is straightforward to locate the minimum energy structure for the dimer-terminated Mo edge, this is not the case for the S edge, as there are many local minima. We have reinvestigated some configurations and find that the two most stable structures are the one described in ref 54 and one where only every second row of outer S atoms dimerize. Three of the investigated structures are shown in Figure 2.

One can see that the symmetric and unreconstructed termination is about ∼25 kJ/mol per unit of MoS_2 (one lattice constant in the *x*-direction wide) more unstable than both reconstructed terminations. The stabilities of the two reconstructed terminations differ very little and are of the order of magnitude of the accuracy of the DFT calculations. In general, relatively little energy is gained by dimer formation at the S edge, in contrast to the Mo edge, where the dimers are very stable and hard to break. The formation of the second dimer pair even costs a slight amount of energy, or at best is energetically neutral. This is because both dimers have to reorient and tilt, whereas one dimer can remain vertical. These results show that the sulfur atoms at the S edge are not so keen to dimerize or to interact in another way, as they already are fairly saturated by bonding to two Mo atoms. This is certainly one of the reasons why vacancy formation on the S edge is easier than on the Mo edge and why the S edge might therefore be more reactive with respect to sulfur extrusion of molecules via C−S hydrogenolysis.

Using the above results regarding the structure of the different edges, we investigate the stability of the linkages in different positions on the MoS_2 strip to find out about the preferred location of the oxygen linkages. We test initially the following positions for substitution: the outer Mo edge, the next-outer Mo edge, the outer S edge, and the next-outer S edge. These positions are shown in Figure 3. We emphasize that we only

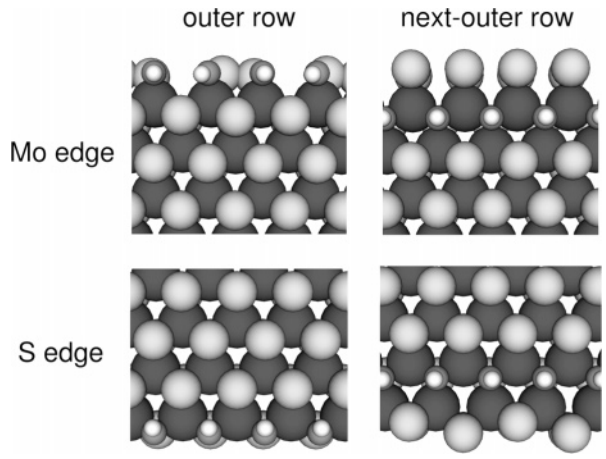

Figure 3. The tested locations for the position of oxygen linkages. All structures are viewed from below, i.e., the *z*-axis points into the paper plane. We have tried to substitute a S atom by OH at both the outer row and the next-outer row at both the Mo edge and the S edge. In this figure, these structures are shown for the case where we substituted S by OH in every unit of MoS_2. We have also tried to only substitute in every second unit, at the same four positions.

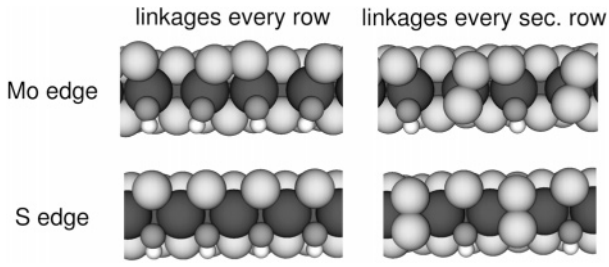

Figure 4. Structures for the presence of linkages either in every unit of MoS_2 or in every second unit. The view is from the side. Only the structures where the linkages are located in the outer row are shown.

TABLE 1: Stability of Oxygen Linkages at Different Locations in the MoS_2 Stripe[a]

position of OH group	linkages every row [kJ/mol]	linkages every second row [kJ/mol]
outer row at Mo edge	0	0
second row at Mo edge	89	25
second row at S edge	52	7
outer row at S edge	−152	−63

[a] All energies are given in kJ/mol. All energies are given per unit cell, i.e., per two rows of MoS_2. The structures with linkages at the outer row at the Mo edge are taken as reference positions, and all energies are reported with respect to these structures.

compare the stability of the structures oxygen linkages at different positions. We do not consider the formation of the OH linkages and the associated reaction energy; this is done in section 3.2.

We performed these calculations for a model, where there are two linkages per unit cell, that is, there is a linkage in every unit, and for a model, where there is one linkage per unit cell, that is, where they are located with one unit of unaltered MoS_2 in between. By this, we cannot only determine the structural and chemical changes at the site with an oxygen linkage, but we can also assess whether the linkages disturb the surroundings and whether there is a tendency for an ordering of the linkages. Selected structures for both substitutions in every row and in every second row are shown in Figure 4.

It is clear from Table 1 that the formation of oxygen linkages in the next-outer rows requires more energy than substitution at the outermost rows, that is, at the edges. This is to be expected, as at the edges there can be reconstructions, whereas this is practically impossible within the basal plane structure. Also, other calculations[44,48,50,54] and measurements[75] confirm the inertness of the basal plane.

Furthermore, one can infer from Table 1 that formation of oxygen linkages are clearly preferred on the S edge compared to the Mo edge. The trend is the same when all the edge units are substituted and when every second unit is substituted. This can be understood in view of the above discussion. At the Mo edge, any disruption of the periodic structure is costly, as reconstructions take place in a concerted manner and have to involve the entire edge. This effect might not be so strong for small clusters, as they only have short edges. Furthermore, the sulfur dimers terminating the edge bind rather strongly. To establish Mo−O−Al linkages, one has to split these dimers, and this energy cost shows up in the stability. On the contrary, on the S edge it is relatively easy to create Mo−O bonds, as reconstructions only take place locally. Therefore, the linkages are expected to be located at the S edge.

In Figure 3, it can be seen that for all four positions, the oxygen linkages are oriented approximately perpendicular to the plane of the MoS_2 sheets. In the alumina support systems, this might have to change slightly, as steric influences might force the linkages into another angle. However, this effect will be similar for all the structures and introduces most probably no change in the relative stabilities of the different structures. On the other hand, it is not sure that the perpendicular configuration of the oxygen linkages actually has to be modified, as there seems to be enough space for them in our model. This would mean that the MoS_2 sheets might actually be able to lie flat on the alumina support and maintain Mo−O−Al linkages. Thereby, they might be able to gain some additional stability from van der Waals interactions with the support. This flat morphology has in fact been observed in microscopy studies.[2,33]

Another interesting result is that the stability for two linkages per unit cell (−152 kJ/mol) is larger than twice the stability for one linkage per cell (−126 kJ/mol), where the linkages are spaced with one unit of MoS_2 in between. This means that there could be a tendency for the oxygen linkages to segregate and to appear in groups.

The main result that oxygen linkages primarily are located at the S edge, however simple the model may be, explains several experimental observations, which have not been explained so far. In the previous high-temperature sulfidation studies of the Type I to Type II transition,[9,20] it was observed that as the temperature increases, the MoS_2 crystals grow and lose edge sites. At a certain temperature, the crystals have grown to an extent where the capacity to accommodate the Co atoms has been reached. Further crystal growth resulted in the segregation of the excess amount of Co as Co_9S_8. It is interesting that the Type I−Type II transition occurred at the temperature where edge saturation by Co had been reached. In accordance with this, the Type I−Type II transition occurred at higher temperatures for samples which initially had a low coverage of the MoS_2 edges by Co, and for unpromoted samples the transition was not observed at all in the temperature region employed. Also, in a recent study[17] unpromoted MoS_2 Type II structures were only observed when either using complexing agents or by use of a carbon support instead of alumina. For supported catalysts, similar effects of complexing agents and supports have been reported.[20,21,23−25]

The present results have provided a much better basis for understanding these observations. There is a strong preference for bonding to the support at the S-edges of MoS_2. Recent DFT

calculations[44,76] and STM observations[77] have shown that the Co atoms also have a preference to be located at specific sites at the S-edges. Thus, there is a strong competition between the Co promoter atoms and the linkages to the support, and for S edges saturated with Co no further bonding via Mo−O−Al is possible.

Thus, our result that oxygen linkages are mainly located at the S edge accounts for several experimental observations of Type I/Type II structures. We can of course not exclude that effects such as the varying pretreatment and preparation parameters of the different studies play a role, but in general, the agreement seems convincing.

Another interesting implication of our results is related to oxygen titration of MoS_2 edge sites. This technique is often used to gain detailed information of the edge sites.[2] Our results suggest that this method may under certain conditions titrate preferentially the S edge and therefore not provide information about the total edge dispersion as assumed in many previous studies (see, e.g., ref 2).

Several previous DFT studies have addressed the support interaction between MoS_2 and alumina. Faye et al.[63,64] investigated the adsorption of MoS_2 sheets on a simplified model for the alumina support and found that the optimal position for the sheet is slightly tilted compared to the perpendicular position. Ionescu et al.[65] studied the adsorption of MoS_2 sheets on several alumina surfaces and found that the optimal adsorption position of the sheet is perpendicular to the alumina surface. These studies have in common that they all consider adsorption of the Mo $(10\bar{1}0)$ surface, which is not terminated by sulfur dimers, as in Figure 1. This "stripped" Mo edge is highly reactive, but is only present under highly reducing conditions. Under normal hydrotreating conditions, this structure is not expected to be present, as shown by DFT results[44] and extrapolation of such results to realistic chemical potentials.[54,59] In addition to this, a stripped Mo edge, that is, a Mo edge not terminated by sulfur, has never been observed in STM studies of the MoS_2 and Co−Mo−S nanocrystals.[39,77] In contrast to the abovementioned studies,[63−65] we find that oxygen linkages are most likely formed on the sulfur $(\bar{1}010)$ edge, which as a starting point is terminated by sulfur dimers. Another argument in favor of the sulfur edges as bonding site to the alumina support is that it explains the abovementioned effect of Co on the Type I−Type II transition temperature. As it is suggested that under sulfiding conditions Co is preferentially located at the sulfur $(\bar{1}010)$ edge,[44,76,77] bonding via the molybdenum edge would not explain the influence of Co on the Type I−Type II transition.

3.2 Creation of Support Linkages. One important aspect of the support interaction is how much energy it actually requires to form and break an Al−O−Mo link. It is known that hydrogen readily adsorbs on the dimer-terminated S edge (see Table 3 and ref 54). Furthermore, there are OH groups present on the alumina support (see, e.g., ref 78). Therefore, the formation of linkages can be treated by the following reaction equation:

$$X{-}OH + (MoS_2){-}SH \rightarrow X{-}O{-}(MoS_2) + H_2S \text{ with } X = Al_2O_3, H$$

The real system with alumina support corresponds to the case $X = Al_2O_3$, but in this paper we consider only the simplified case with $X = H$. From our results, we calculate that the formation of two linkages per unit cell requires $\Delta E = 117$ kJ/mol and the formation of one linkage per unit cell requires $\Delta E = 61$ kJ/mol. Thus, the linkages are thermodynamically unstable and it takes energy to create them. However, the fact that they may be present under operating conditions is probably related to their presence in the oxidic precursor structures[2] and it indicates that there is a kinetic barrier associated with their rupture.

The validity of our model depends on the difference between the two situations with $X = H$ and $X = Al_2O_3$. As discussed in section 2, the vibrational frequencies of OH groups on thin alumina films and in water are very similar. Therefore, we have good reason to believe that our model is a reasonable approximation.

3.3 Vacancy Formation. It is generally believed that vacancy formation plays a key role in hydrotreating catalysis, as this provides reactive sites (see ref 2). It has been speculated that sulfur extrusion primarily takes place at the S edge, as it is much easier to create vacancies there compared to the Mo edge.[54] Thus, an important prerequisite for the S edge to be reactive is the observation that vacancies can be formed easily.[35,43,44,50,79] This is definitely the case for the unaltered S edge, where we in the present study find that the formation of a single vacancy only requires an energy of 26 kJ/mol. Forming two vacancies per unit cell, that is, at the whole edge, requires 86 kJ/mol. These results reproduce the results of Bollinger et al.,[54] who found energies of 22 kJ/mol and 84 kJ/mol, respectively. The energy required for a single vacancy is definitely accessible under hydrotreating conditions, and therefore, vacancies can be formed easily.

We proceed to investigate vacancy formation on the S edge with linkages present in every unit and in every second unit. The investigated structures are shown in Figure 5. To calculate the energies for vacancy formation, we use the following equation:

$$\Delta E_{vac} = E[MoS_2 + n(*)] + nE[H_2S] - E[MoS_2 + nS(*)] - nE[H_2]$$

where n is the number of S atoms removed per unit cell and $E[H_2S]$ and $E[H_2]$ are the energies of H_2S and H_2 in the gas phase. In the above equation, MoS_2 does not only denote the structure without linkages, but also the structures where linkages are present.

As one can see in Table 2, the presence of oxygen linkages changes the possibility for vacancy formation dramatically. On the S edge with linkages present in every unit of MoS_2, vacancy formation is virtually impossible with an energy cost of 153 kJ/mol for one vacancy and 292 kJ/mol for two vacancies. A very interesting case is the S edge, where an oxygen linkage is present in every second unit. On the edge sites, where linkages are present, vacancy formation requires approximately the same energy as for the S edge with linkages in every unit. Also on the edge sites, where no linkages are present, vacancy formation is endothermic with 67 kJ/mol and therefore more difficult, and it requires 41 kJ/mol more energy and on a S edge without any linkages. This shows clearly that the oxygen linkages not only prevent formation of vacancies in the unit, where they are located, but they can also prevent formation of vacancies in the neighboring unit.

This result could be a key factor for the reduced reactivity of the Type I structures, where Mo−O−Al linkages to the alumina support are present. Vacancy formation is a key prerequisite for catalytic activity, and a vacancy formation energy of 153 kJ/mol renders the edge sites with linkages basically inert.

3.4 Electronic Properties of the MoS_2-Based Structures with Linkages. In many previous studies, catalytic activity has

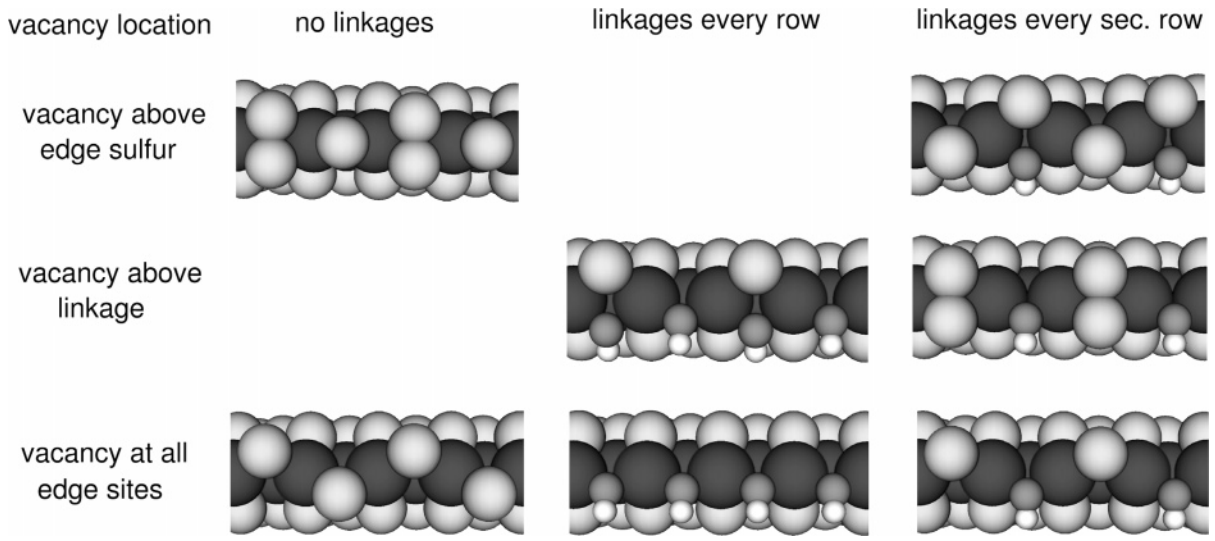

Figure 5. Investigated structures for vacancy formation. All structures are calculated energy minima.

TABLE 2: Energies for Vacancy Formation on the OH-Substituted S Edge[c]

vacancy location	no linkages [kJ/mol]	linkages every row [kJ/ mol]	linkages every second row [kJ/mol]
vacancy above edge sulfur	26		67
vacancy above linkage		153	139[b]
vacancies at all edge sites	86	290[a]	168

[a] Residual force is 0.13 eV/Å. [b] Residual force 0.12 eV/Å. Energy changes were less than in 1 kJ/mol in last 30 steps, therefore the relaxations were terminated. [c] All energies are given in kJ/mol. All energies are given per unit cell, i.e., per two rows of MoS_2.

been correlated with metal−sulfur bonding energies (see, e.g., refs 2 and 44). Recent studies suggest that also the metallic edge states at both the Mo and the S edges might play a role.[39,53,54] Therefore, changes in the electronic structure of the S edge introduced by the linkages may have important consequences for the reactivity. For example, it is interesting to know whether the metallic edge state present at the S edge[54] is still present when oxygen linkages are introduced. Furthermore, the shape of the Kohn−Sham wave functions of these edge states is of interest, as one can see, if they are located at the sites of the S edge, where thiolate and other probe molecules may bind.

In Figure 6, the band structure and wave functions of edge states are shown for the three cases considered in this paper: The S edge without any linkages, the S edge with linkages in every unit, and the S edge with linkages in every second unit. The electronic structure of the S edge without any linkages has been studied in ref 54. We have reproduced those results for comparison and all our results of the S edge without linkages agree with the ones by Bollinger et al.[54] Furthermore, we use the same nomenclature for the metallic edge states as in ref 54. For all three structures, the two previously found edge states at the Mo edge (i.e., the edge that does not contain linkages), which are denoted I and II are present and are reproduced as in ref 54.

All three structures have two common edge states crossing the Fermi levels denoted by I and II. The structure without linkages and the structure with linkages in every row also have a metallic edge state located at the S edge. For the S edge without linkages, the edge state IIIa is mainly characterized by the d−d bonds of the outermost Mo atoms, but there is also some p−d bonding between the outermost Mo atoms and the S atoms at the edge. The metallic edge state IIIb for the S edge with linkages in every unit is mainly characterized by p−d bonds of the upper S atom and the Mo atom behind and p−p bonding between the S atoms at the edges. The S edge with linkages in every second unit does not have any metallic edge state, as the corresponding band (the one with IIIc marked) does not cross the Fermi level. However, near the Γ-point, this band comes close to the Fermi level, although one can clearly see that it does not reach it. This state is marked by IIIc and is plotted as well. It is dominated by p−p bonds between the S and Mo atoms.

In general, it is clearly visible that by the presence of the linkages, the edge state at the S edge is either eliminated or severely disturbed. Most probably, this means that the reactivity of the S edge is changed by the linkages. One can also see that the presence of a linkage not only locally changes the electronic structure, but that it also induces changes of the electronic structure in its surroundings. In particular, the presence of linkages in every second unit seems to destroy the metallic edge state.

3.5 Hydrogen Adsorption at the S Edge in the Presence of Oxygen Linkages. Another important aspect for the reactivity of the S edge is its ability to adsorb hydrogen, as it is needed for sulfur extrusion. Hydrogen adsorption on the S edge without oxygen linkages is exothermic (see also ref 54) so that there is hydrogen present on the S edge under sulfiding conditions. Although in the previous section it was found that the high energy for vacancy formation probably prevents the S edge with linkages to be reactive, it would nonetheless be interesting to know whether hydrogen is present on the S edge with linkages during the hydrotreating process. We calculate the adsorption energy for hydrogen according to the following equation:

$$\Delta E_{\mathrm{Hydrogen}} = E[MoS_2 + n\mathrm{H}] - E[MoS_2] - n/2 \cdot E[H_2]$$

where n is the number of adsorbed hydrogen atoms per unit cell and $E[H_2]$ is the energy of H_2 in the gas phase. Again, MoS_2 does not only denote a unit cell of the structure, where no linkages are present, but also the structures with linkages.

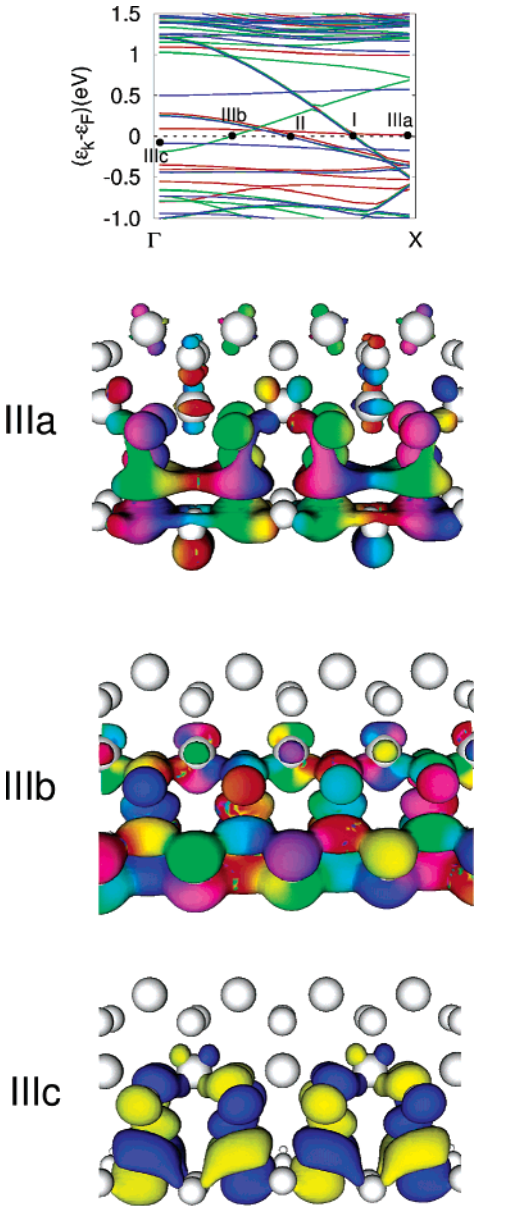

Figure 6. The one-dimensional band structure and the contours of the Kohn−Sham wave functions for three structures: The S edge without any linkages, the S edge with linkages in every unit, and the S edge with linkages in every second unit. The color code for the band-structure plot is red, S edge without any linkages; green, S edge with linkages in every unit; and blue, S linkages in every second unit. The linkages are located at the outermost edge, as in the two lowest structures in Figure 4. For all three systems, edge states I and II, which are localized at the Mo edge (same notation as in ref 54), are present. Edge state IIIa belongs to the structure without any linkages and is localized on the S edge. The structure with linkages in every unit also has an edge state localized at the S edge, which is denoted IIIb. The structure with linkages in every second unit does not have an edge state at the S edge, as no band with wave functions localized at the S edge crosses the Fermi level. However, there is one band which is very close to the Fermi level at the Γ-point. This state is marked as IIIc and the corresponding wave function is also shown. The contours of the Kohn−Sham wave functions are colored according to the phase of the wave functions.

The investigated structures are shown in Figure 7. First, we examine the S edge without linkages. We find energies of −52 kJ/mol and −112 kJ/mol for the adsorption of one and two H atoms, respectively, which agree reasonably well with the energies of −59 kJ/mol and −122 kJ/mol found by Bollinger et al.

We investigate hydrogen adsorption both for the structure with linkages in every unit and linkages in every second unit. The hydrogen adsorption energies are listed in Table 3.

From Table 3, one can see that hydrogen adsorption on the S edge with oxygen linkages present in every unit is slightly exothermic for one H atom per unit cell and endothermic for two H atoms per unit cell. In contrast to the vacancy formation, the oxygen linkages do not affect significantly the hydrogen adsorption on the neighboring rows, as hydrogen adsorption is still exothermic there. In fact, it is even more exothermic than on the S edge without any linkages. Therefore, we can conclude that hydrogen adsorption on the edge sites, where linkages are present, is only slightly exothermic, whereas hydrogen adsorption on the edge sites without linkages is clearly exothermic. Thus, one would certainly expect hydrogen to be present on all edge sites without linkages, no matter whether the neighboring edge sites have linkages or not.

In summary, hydrogen adsorption is not nearly affected as drastically as vacancy formation and is likely to occur, at least on edge sites, where no linkages are present, but under certain partial hydrogen pressures also on edge sites with linkages. However, without the presence of vacancies, this adsorbed hydrogen cannot be used for sulfur extrusion and is therefore probably not of direct relevance. Therefore, adsorbed hydrogen is probably not important for edges where most rows form linkages to the alumina.

4. Conclusion

The present DFT calculations have provided new insight regarding the nature and the influence of oxygen linkages between MoS_2-type nanocrystals and a support. The results provide also a better basis for understanding the catalytic properties of Type I and Type II structures. In summary, we have shown that oxygen linkages are predominantly present on the outer $(\bar{1}010)$ sulfur edge, as they are more stable here than at any other possible position. The results also show that the oxygen linkages are oriented approximately perpendicular to the plane of the MoS_2 sheets. This might imply that MoS_2 sheets may lie flat on the alumina support and maintain the oxygen linkages. The preference for the oxygen linkages to be located at the sulfur edge has also strong implications for the important Co (Ni) promoted catalysts, since the most favorable location of the Co atoms also is on the outer S edge.[44] This means that the formation of linkages competes strongly with the incorporation of Co into the S edge. If the S edge is saturated with Co, no further formation of linkages to the support is likely to happen. Consequently, the more Co is present in the S edge (up to the limit, where it segregates into Co_9S_8) the lower the temperature for the Type I−Type II transition is expected to be, in accord with previous observations.[9] Thus, our result that the linkages most probably are only present at the S edge is consistent with the fact that Co is favored to be incorporated at the S edge and that the temperature of the Type I−Type II transition depends on the amount of Co present.

The present results suggest that the oxygen linkages between the MoS_2-type structures and the support are not stable as such (i.e., the reaction considered in section 3.2. for the formation of linkages is endothermic). This allows one to understand the observations showing that by proper choice of preparation parameters, one may synthesize the more active Type II structures directly.[21−25] The fact that the Type I structures may survive the reducing environment encountered under hydrotreating suggests that once Mo−O−Al linkages are formed, the activation energy involved in the breakage is quite high.

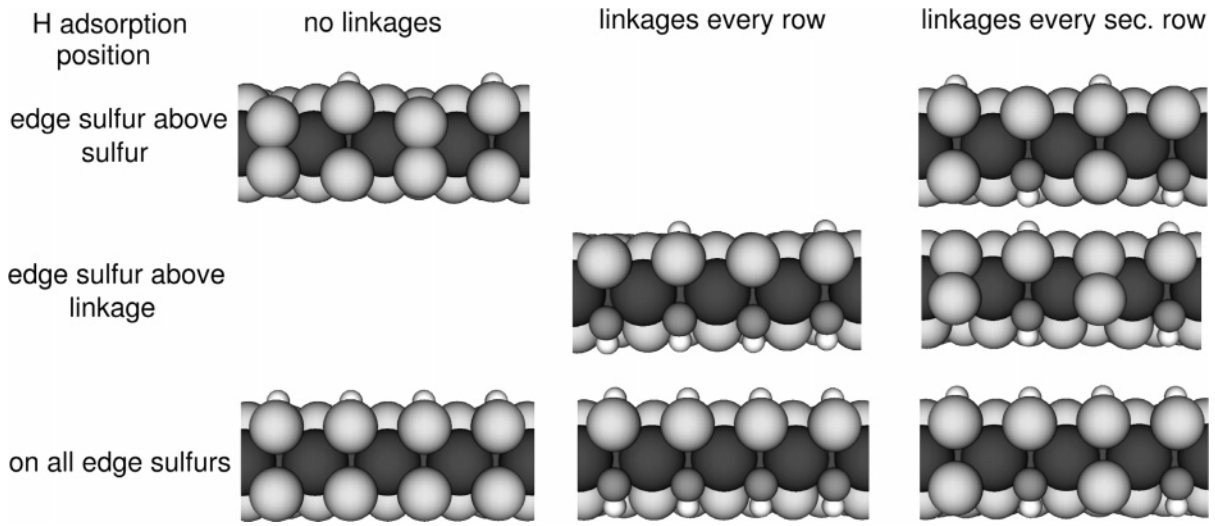

Figure 7. Investigated structures for hydrogen adsorption on the S edge without linkages, linkages in every unit, and linkages in every second unit. All structures are calculated energy minima.

TABLE 3: Energies for Hydrogen Adsorption on the OH-Substituted S Edge[a]

H adsorption position	no linkages [kJ/mol]	linkages every row [kJ/mol]	linkages every second row [kJ/mol]
edge sulfur above edge sulfur/no linkage	−52		−73
edge sulfur above linkage		−5	3
on all edge sulfurs	−112	27	−69

[a] All energies are given in kJ/mol. All energies are given per unit cell, i.e., per two rows of MoS_2.

Our results show clearly that both the structure and the reactivity of S edges are severely modified by the formation of oxygen linkages. The formation of vacancies becomes very endothermic (153 kJ/mol for one vacancy) so that it is practically impossible under working conditions. Many previous studies[35,43,44,50,78] have shown that vacancy formation is a key step in the hydrodesulfurization process. Therefore, one can assume that the reactivity of the S edge with linkages is severely reduced. A very interesting result is that the presence of linkages not only disables vacancy formation in the row where it is located but that it also makes vacancy formation on the sulfur edge site adjacent to the site with the linkage more difficult. This will also be the case if the adjacent site contains a Co atom. The increased endothermicity of vacancy formation is a central result of this work, which may be one of the reasons why Type I structures have a lower catalytic activity than Type II structures. In the Introduction and in the previous section, it has been argued that the Type I−Type II transition is associated with the breaking of Mo−O−Al linkages and that in Type I structures those linkages are present. We have now shown that these linkages are present on the S edge and that they reduce reactivity by making it very hard, if not impossible, to form vacancies, which are necessary for sulfur extrusion reactions. Thus, we have obtained a consistent picture about the catalytic influence of oxygen linkages in the MoS_2 structure. It is seen that the present results explain nicely the changes in Type I to Type II transition behavior observed in previous studies.[2,9]

A third issue we have investigated is the adsorption of hydrogen. Here, we find that the adsorption of hydrogen on edge sites above linkages is only slightly exothermic (−5 kJ/mol) compared to −52 kJ/mol on the S edge sites without linkages. The adsorption of hydrogen on a site neighboring to an edge site with a linkage is significantly more exothermic with −73 kJ/mol. These results may for some reactions affect the hydrogenation steps. They could also be significant for situations where only few linkages are present and reactivity is retained. There, it might not be very advantageous that the exothermicity of hydrogen adsorption increases. It is important that hydrogen adsorption is exothermic so that it is available on the edge during hydrodesulfurization. On the other hand, the adsorption of hydrogen should not be too exothermic, as it is then too strongly bound to the edge and it is less accessible for catalytic processes. Judging the precise influence of the changes in hydrogen adsorption is complicated and depends on the exact conditions. However, for the present work this is only of minor importance, as the main factor leading to a reduced reactivity is the significantly increased energy necessary for the formation of vacancies.

This study has focused on how the presence of oxygen linkages to a support may influence the intrinsic properties of MoS_2 and Co−Mo−S type structures. The simple model introduced is apparently able to provide valuable insight into many such phenomena. It is evident that if one is to gain insight into steric effects caused by the support, more elaborate models for the sulfide-support system must be introduced.

Acknowledgment. We acknowledge support from the Danish Center for Scientific Computing through grant no. HDW-1101-05.

References and Notes

(1) Boudart, M. *Adv. Catal.* **1969**, *20*, 153.

(2) Topsøe, H.; Clausen, B. S.; Massoth, F. E. In *Hydrotreating Catalysis − Science and Technology*; Anderson, J. R., Boudart, M., Eds.; Springer-Verlag: Berlin, 1996; Vol. 11.

(3) Breysse, M.; Afanasiev, P.; Geantet, C.; Vrinat, M. *Catal. Today* **2003**, *86*, 5.

(4) Song, C. *Catal. Today* **2003**, *86*, 211.

(5) Whitehurst, D. D.; Isoda, T.; Mochida, I. *Adv. Catal.* **1998**, *42*, 345.

(6) Knudsen, K. G.; Cooper, B. C.; Topsøe, H. *Appl. Catal., A* **1999**, *189*, 205.

(7) Landau, M. V. *Catal. Today* **1997**, *36*, 393.

(8) Clausen, B. S.; Topsøe, H.; Candia, R.; Villadsen, J.; Lengeler, B.; Als-Nielsen, J.; Christensen, F. *J. Phys. Chem.* **1982**, *85*, 3868.
(9) Candia, R.; Villadsen, J.; Topsøe, N.-Y.; Clausen, B. S.; Topsøe, H. *Bull. Soc. Chim. Belg.* **1984**, *93*, 763.
(10) Ratnasamy, P.; Knözinger, H. *J. Catal.* **1978**, *54*, 155.
(11) Topsøe, N.-Y. *J. Catal.* **1980**, *64*, 235.
(12) van Veen, J. A. R.; Hendriks, P. A. J. M.; Romers, E. J. G. M.; Andréa, R. R. *J. Phys. Chem.* **1990**, *94*, 5275.
(13) Topsøe, N.-Y.; Topsøe, H. *J. Catal.* **1993**, *139*, 631.
(14) Li, C. P.; Hercules, D. M. *J. Phys. Chem.* **1984**, *88*, 456.
(15) Arnoldy, P.; van den Heijkant, J. A. M.; de Book, G. D.; Moulijn, J. A. *J. Catal.* **1985**, *92*, 35.
(16) Derouane, E. G.; Pedersen, E.; Clausen, B. S.; Gabelica, Z.; Candia, R.; Topsøe, H. *J. Catal.***1986**, *99*, 253.
(17) Hensen, E. J. M.; de Beer, V. H. J.; van Veen, J. A. R.; van Santen, R. A. *Catal. Lett.* **2002**, *84*, 59.
(18) Leliveld, R. G.; van Dillen, A. J.; Geus, J. W.; Koningsberger, D. C. *J. Catal.* **1997**, *165*, 184.
(19) Diemann, E.; Weber, Th.; Müller, A. *J. Catal.* **1994**, *148*, 288.
(20) Topsøe, H.; Candia, R.; Topsøe, N.-Y.; Clausen, B. S. *Bull. Soc. Chim. Belg.* **1984**, *93*, 783.
(21) van Veen, J. A. R.; Gerkema, E.; van der Kraan, A. M.; Knoester, A. *J. Chem. Soc. Chem. Commun.* **1987**, 1684.
(22) Scheffer, B.; Arnoldy, P.; Moulijn, J. A. *J. Catal.* **1988**, *112*, 516.
(23) Medici, L.; Prins, R. *J. Catal.* **1996**, *163*, 38.
(24) Coulier, L.; Kishan, G.; van Veen, J. A. R.; Niemantsverdriet, J. W. *J. Phys. Chem. B* **2002**, *106*, 5897.
(25) Sun, M.; Nicosia, D.; Prins, R. *Catal. Today* **2003**, *86*, 173.
(26) Topsøe, H.; Clausen, B. S.; Burriesci, N.; Candia, R.; Mørup, S. *Stud. Surf. Sci. Catal.* **1979**, *3*, 479.
(27) Breysse, M.; Bennett, B. A.; Chadwick, D.; Vrinat, M. *Bull. Soc. Chim. Belg.* **1981**, *90*, 1271.
(28) Vissers, J. P. R.; Scheffer, B.; de Beer, J. H. J.; Moulijn, J. A.; Prins, R. *J. Catal.* **1987**, *105*, 277.
(29) Okamoto, Y.; Ochiai, K.; Kawano, M.; Kobayashi, K.; Kubota, T. *Appl. Catal., A* **2002**, *226*, 115.
(30) Hayden, T. F.; Dumesic, J. A. *J. Catal.* **1987**, *103*, 385.
(31) Hayden, T. F.; Dumesic, J. A.; Sherwood, R. D.; Baker, T. K. *J. Catal.* **1987**, *105*, 299.
(32) Sakashita, Y.; Yoneda, T. *J. Catal.* **1999**, *185*, 487.
(33) Kooyman, P. J.; Buglass, J. G.; Reinhoudt, H. R.; van Langefeld, A. D.; Hensen, E. J. M.; Zandbergen, H. W.; van Veen, J. A. R. *J. Phys. Chem. B* **2002**, *106*, 11795.
(34) Shimada, H. *Catal. Today* **2003**, *86*, 17.
(35) Nørskov, J. K.; Clausen, B. S.; Topsøe, H. *Catal. Lett.* **1992**, *13*, 1.
(36) Daage, M.; Chianelli, R. R. *J. Catal.* **1994**, *149*, 414.
(37) Molina, L. M.; Hammer, B. *Phys. Rev. Lett.* **2003**, *90*, 206102.
(38) Helveg, S.; Lauritsen, J. V.; Lægsgaard, E.; Stensgaard, I.; Nørskov, J. K.; Clausen, B. S.; Topsøe, H.; Besenbacher, F. *Phys. Rev. Lett.* **2000**, *84*, 951.
(39) Lauritsen, J. V.; Nyberg, M.; Vang, R. T.; Bollinger, M. V.; Clausen, B. S.; Topsøe, H.; Jacobsen, K. W.; Lægsgaard, E.; Nørskov, J. K.; Besenbacher, F. *Nanotechnology* **2003**, *14*, 385.
(40) Gates, B. G.; Topsøe, H. *Polyhedron* **1997**, *16*, 3213.
(41) Neurock, M.; van Santen, R. A. *J. Am. Chem. Soc.* **1994**, *116*, 4427.
(42) Neurock, M. *Appl. Catal., A* **1997**, *160*, 169.
(43) Byskov, L. S.; Hammer, B.; Nørskov, J. K.; Clausen, B. S.; Topsøe, H. *Catal. Lett.* **1997**, *47*, 177.
(44) Byskov, L. S.; Nørskov, J. K.; Clausen, B. S.; Topsøe, H. *J. Catal.* **1999**, *187*, 109.
(45) Byskov, L. S.; Bollinger, M.; Nørskov, J. K.; Clausen, B. S.; Topsøe, H. *J. Mol. Catal. A* **2000**, *163*, 117.
(46) Raubaud, P.; Hafner, J.; Kresse, G.; Toulhoat, H. *Surf. Sci.* **1998**, *407*, 237.
(47) Raybaud, P.; Hafner, J.; Kresse, G.; Toulhoat, H. *Phys. Rev. Lett.* **1998**, *80*, 1481.
(48) Raybaud, P.; Hafner, J.; Kresse, G.; Kasztelan, S.; Toulhoat, H. *J. Catal.* **2000**, *189*, 129.
(49) Raybaud, P.; Hafner, J.; Kresse, G.; Kasztelan, S.; Toulhoat, H. *J. Catal.* **2000**, *190*, 128.
(50) Cristol, S.; Paul, J. F.; Payen, E.; Bougeard, D.; Hafner, J.; Hutschka, F. In *Hydrotreatment and Hydrocracking of Oil Fractions*; Delmon, B., Froment, F. G., Grange, P., Eds.; Elsevier: Amsterdam, The Netherlands, 1999; p 327.
(51) Cristol, S.; Paul, J. F.; Payen, E.; Bougeard, D.; Clémendot, S.; Hutschka, F. *J. Phys. Chem. B* **2000**, *104*, 11220.
(52) Christol, S.; Paul, J. F.; Payen, E. *J. Phys. Chem. B* **2002**, *106*, 5659.
(53) Bollinger, M. V.; Lauritsen, J. V.; Jacobsen, K. W.; Nørskov, J. K.; Helveg, S.; Besenbacher, F. *Phys. Rev. Lett.* **2001**, *87*, 19.
(54) Bollinger, M. V.; Jacobsen, K. W.; Nørskov, J. K. *Phys. Rev. B* **2003**, *67*, 085410.
(55) Alexiev, V.; Prins, R.; Weber, T. *Phys. Chem. Chem. Phys.* **2001**, *3*, 5326.
(56) Travert, A.; Dujardin, C.; Maugé, F.; Cristol, S.; Paul, J. F.; Payen E.; Bougeard, D. *Catal. Today* **2001**, *70*, 255.
(57) Travert, A.; Nakamura, H.; van Santen, R. A.; Cristol, S.; Paul, J. F.; Payen, E. *J. Am. Chem. Soc.* **2003**, *124*, 70.
(58) Paul, J. F.; Payen, E. *J. Phys. Chem. B* **2003**, *107*, 4057.
(59) Schweiger, H.; Raybaud, P.; Kresse, G.; Toulhoat, H. *J. Catal.* **2002**, *207*, 76.
(60) Spirko, J. A.; Neiman, M. L.; Oelker, A. M.; Klier, K. *Surf. Sci.* **2003**, *542*, 192.
(61) Faye, P.; Payen, E.; Bougeard, D. In *Hydrotreatment and hydrocracking of oil fractions*, Froment, G. F., Delmon, B., Grange, P., Eds.; Elsevier: Amsterdam, The Netherlands, 1997.
(62) Miura, R.; Gunji, I.; Kanougi, T.; Endou, A.; Kubo, M.; Chartterjee, A.; Miyamoto, A.; Yokomichi, Y.; Nakazono, Y.; Yoneda, T. Abstracts of papers of the American Chemical Society **1998**, *216*, U600-U601 018-PETR Part 2.
(63) Faye, P.; Payen, E.; Bougeard, D. *J. Catal.* **1998**, *179*, 560.
(64) Faye, P.; Payen, E.; Bougeard, D. *J. Catal.* **1999**, *183*, 396.
(65) Ionescu, A.; Allouche, A.; Aycard, J.-P.; Rajzmann, M.; Gall, R. L. *J. Phys. Chem. B* **2003**, *107*, 8490.
(66) The program *dacapo* can be obtained freely at http://www.fysik.dtu.dk.
(67) Hammer, B.; Hansen, L. B.; Nørskov, J. K. *Phys. Rev. B* **1999**, *59*, 7413.
(68) Kresse, G.; Furthmüller, J. *Comput. Mater. Sci.* **1996**, *6*, 15.
(69) Vanderbilt, D. *Phys. Rev. B* **1990**, *41*, 7892.
(70) Laasonen, K.; Pasquarello, A.; Car, R.; Lee, C.; Vanderbilt, D. *Phys. Rev. B* **1993**, *47*, 10142.
(71) Monkhorst, H. J.; Pack, J. D. *Phys. Rev. B* **1976**, *13*, 5188.
(72) Perdew, J. P.; Chevary, J. A.; Vosko, S. H.; Jackson, K. A.; Pederson, M. R.; Singh, D. J.; Fiolhais, C. *Phys. Rev. B* **1992**, *46*, 6671.
(73) *CRC Handbook of Chemistry and Physics*, 83th ed.; Lide, D. R., Ed.; CRC Press: Boca Raton, FL, 2002.
(74) Layman, K. A.; Hemminger, J. C. *J. Catal.* **2004**, *222*, 207.
(75) Salmeron, M.; Somorjai, G. A.; Wold, A.; Chianelli, R.; Liang, K. S. *Chem. Phys. Lett.* **1982**, *90*, 105.
(76) Schweiger, H.; Raybaud, P.; Toulhoat, H. *J. Catal.* **2002**, *212*, 33.
(77) Lauritsen, J. V.; Helveg, S.; Lægsgaard, E.; Stensgaard, I.; Clausen, B. S.; Topsøe, H.; Besenbacher, F. *J. Catal.* **2001**, *197*, 1.
(78) Heinrich, V. E.; Misra, C. *The Surface Science of Metal Oxides*; Cambridge University Press: Cambridge, MA, 1994.
(79) Raybaud, P.; Hafner, J.; Kresse, G.; Toulhoat, In *Hydrotreatment and Hydrocracking of Oil Fraction;* Delmon, B., Froment, G. F., Grange, P., Eds.; Elsevier: Amsterdam, The Netherlands, 1999; p 309.